The EMBO Journal (2012) 31, 2498–2510 | © 2012 European Molecular Biology Organization | All Rights Reserved 0261-4189/12
www.embojournal.org

THE EMBO JOURNAL

Genetic inactivation of Cdk7 leads to cell cycle arrest and induces premature aging due to adult stem cell exhaustion

Miguel Ganuza[1], Cristina Sáiz-Ladera[2], Marta Cañamero[3], Gonzalo Gómez[4], Ralph Schneider[5], María A Blasco[5], David Pisano[4], Jesús M Paramio[2], David Santamaría[1,*] and Mariano Barbacid[1,*]

[1]Experimental Oncology, Molecular Oncology Programme, Centro Nacional de Investigaciones Oncológicas (CNIO), Madrid, Spain, [2]Department of Basic Research, Molecular Oncology Unit, CIEMAT, Madrid, Spain, [3]Comparative Pathology Unit, Biotechnology Programme, Centro Nacional de Investigaciones Oncológicas (CNIO), Madrid, Spain, [4]Bioinformatics Unit, Structural Biology and Biocomputing Programme, Centro Nacional de Investigaciones Oncológicas (CNIO), Madrid, Spain and [5]Telomeres and Telomerase Group, Molecular Oncology Programme, Centro Nacional de Investigaciones Oncológicas (CNIO), Madrid, Spain

Cyclin-dependent kinase (Cdk)7, the catalytic subunit of the Cdk-activating kinase (CAK) complex has been implicated in the control of cell cycle progression and of RNA polymerase II (RNA pol II)-mediated transcription. Genetic inactivation of the *Cdk7* locus revealed that whereas Cdk7 is completely dispensable for global transcription, is essential for the cell cycle via phosphorylation of Cdk1 and Cdk2. *In vivo*, *Cdk7* is also indispensable for cell proliferation except during the initial stages of embryonic development. Interestingly, widespread elimination of Cdk7 in adult tissues with low proliferative indexes had no phenotypic consequences. However, ablation of conditional *Cdk7* alleles in tissues with elevated cellular turnover led to the efficient repopulation of these tissues with Cdk7-expressing cells most likely derived from adult stem cells that may have escaped the inactivation of their targeted *Cdk7* alleles. This process, a physiological attempt to maintain tissue homeostasis, led to the attrition of adult stem cell pools and to the appearance of age-related phenotypes, including telomere shortening and early death.

The EMBO Journal (2012) **31,** 2498–2510. doi:10.1038/emboj.2012.94; Published online 13 April 2012
Subject Categories: signal transduction; cell cycle
Keywords: CAK; Cdk7; *in vivo* elimination; mouse model; stem cell exhaustion

*Corresponding author. D Santamaria or M Barbacid, Experimental Oncology, Molecular Oncology Programme, Madrid, 28029, Spain. Tel.: +34 917328015; Fax: +34 912246980;
E-mail: dsantamaria@cnio.es or mbarbacid@cnio.es.

Received: 22 November 2011; accepted: 20 March 2012; published online 13 April 2012

Introduction

Cell cycle regulation in eukaryotic cells is controlled by a family of conserved heterodimeric serine/threonine kinases made of a regulatory subunit, generically known as Cyclin, and a catalytic component designated as Cyclin-dependent kinase (Cdk) (Malumbres and Barbacid, 2005). Cyclins are essential to activate the catalytic activity of their cognate Cdks and to provide substrate specificity. However, optimal kinase activity requires additional steps, one of which involves phosphorylation of a key threonine residue located within the activating segment, also known as T-loop, of the Cdk subunit (Harper and Elledge, 1998). This activating step is carried out by the Cdk-activating kinase (CAK), a trimeric kinase whose catalytic activity is also provided by a Cdk, known as Cdk7. Cdk7 becomes activated by binding to Cyclin H (CycH) and to a third regulatory subunit known as Mat1 (Harper and Elledge, 1998).

Interestingly, CAK is also a component of the general transcription factor TFIIH, a large protein complex involved in the phosphorylation of serine residues (mainly Ser5) located at the carboxy terminal domain (CTD) of the large subunit of RNA polymerase II (RNA pol II). Thus, CAK has also been implicated in the regulation of promoter clearance and progression of the basic transcriptional machinery (Palancade and Bensaude, 2003). Yet, recent evidence suggests that RNA pol II-mediated transcription may not be overtly affected by the absence of CAK activity. For instance, a temperature-sensitive allele of Mcs6, the corresponding orthologue in *S. pombe*, only affects transcription of a selective cell-division gene cluster, representing $<5\%$ of all transcripts (Lee *et al*, 2005). Similarly, Cdk7 deficiency results in severe mitotic defects in *C. elegans* and *D. melanogaster* without concomitant loss of CTD phosphorylation or transcriptional integrity, respectively (Larochelle *et al*, 1998; Wallenfang and Seydoux, 2002). Finally, mouse cells defective in the regulatory subunit Mat1 present functional *de novo* transcription (Rossi *et al*, 2001). Regardless of its potential role in regulating the cell cycle and/or transcription, genetic studies have shown that *Cdk7* is an essential gene in *D. melanogaster* (Larochelle *et al*, 1998). Likewise, Mat1 or CycH deficiency results in an early embryonic lethality in mice (Rossi *et al*, 2001; Patel and Simon, 2010).

We undertook the present study to analyse the physiological role of Cdk7 in mice by genetic targeting. We report that loss of Cdk7 causes impaired T-loop phosphorylation of cell cycle Cdks, leading to cessation of cell division *in vitro* and early embryonic lethality *in vivo*. In contrast, RNA pol II-mediated transcription is unaffected with the exception of E2F-controlled genes, an indirect consequence of deficient Cdk function. Loss of Cdk7 expression in adult mice has a little effect on non-proliferating tissues. However, elimination of Cdk7 in proliferating tissues leads to the premature onset of age-related phenotypes most likely due

to depletion of progenitor cells and exhaustion of their renewal capacity.

Results

Cdk7 is required for cell proliferation but not for global transcription

Cdk7$^{lox/lox}$ mouse embryonic fibroblasts (MEF) were generated from *Cdk7*$^{lox/lox}$ embryos (see Materials and methods). These MEFs were subsequently infected with adenoviral vectors expressing the Cre recombinase (Ad-Cre) to generate *Cdk7*$^{mut/mut}$ MEFs that lack detectable levels of Cdk7 expression (Supplementary Figure 1). These mutant MEFs failed to proliferate and to enter S phase upon serum stimulation (Supplementary Figure 2A and B). As expected, loss of Cdk7 expression caused degradation of the other CAK subunits, CycH and Mat1 (Supplementary Figure 2C; Rossi *et al*, 2001). Likewise, Cdk7 was also degraded upon shRNA-mediated knockdown of either Mat1 or CycH (data not shown).

Cdk7 is thought to activate transcription by phosphorylating serine residues, mainly Ser5, located within the CTD of RNA pol II (Palancade and Bensaude, 2003). Interestingly, the phosphorylation levels of this residue were unaffected in *Cdk7*$^{mut/mut}$ MEFs (Figure 1A), indicating that either Cdk7 is not involved in the phosphorylation of this critical residue or that this activity can be carried out by another kinase with similar efficiency. This result prompted us to assess whether RNA pol II-mediated transcription was affected in the absence of Cdk7. To this end, 7 days after exposure to Ad-Cre, *Cdk7*$^{mut/mut}$ MEFs were infected with a lentiviral vector expressing a green fluorescent protein (GFP) from a constitutive promoter. After 72 h, the intensity of the GFP reporter in *Cdk7*$^{mut/mut}$ MEFs was comparable to that of *Cdk7*$^{lox/lox}$ controls (Supplementary Figure 2D). Likewise, *Cdk7*$^{mut/mut}$ and *Cdk7*$^{lox/lox}$ MEFs were serum starved in order to match their proliferation rates. Under these conditions the rate of *de novo* protein synthesis, as measured by [^{35}S]methionine incorporation, was not affected in the absence of Cdk7 (Supplementary Figure 2E). All together, these results suggest that Cdk7 is dispensable for *de novo* transcription and translation.

To further characterize the transcriptional status of cells devoid of Cdk7, we compared the gene expression profile of *Cdk7*$^{lox/lox}$ with *Cdk7*$^{mut/mut}$ MEFs by standard microarray analysis. To rule out a possible bias due to their different proliferation rates, we decided to perform a gene set enrichment analysis (GSEA) on a predefined subset of 443 housekeeping genes, as expression of this cluster has been shown to be proliferation-rate independent (Eisenberg and Levanon, 2003). Our results indicated that transcription of this housekeeping gene-set was not statistically altered 10 days after the elimination of Cdk7 (false discovery rate (FDR) 0.339) (Supplementary Figure 2F–H) thus indicating that the inability of *Cdk7*$^{mut/mut}$ MEFs to proliferate was not due to a defect in global transcription. Indeed, when we analysed the entire microarray data set in *Cdk7*$^{mut/mut}$ MEFs (FDR$<$0.05), we detected the upregulation in 1250 genes along with the presence of 1218 additional genes that showed no variation in their levels of expression (data not shown) thus supporting the notion that Cdk7 is dispensable for RNA pol II-mediated global transcription.

Cdk7 is essential for activation of cell cycle Cdks

Cdk7$^{mut/mut}$ MEFs showed no detectable phosphorylation of Thr160, the activating residue in the T-loop of Cdk2 (Figure 1A). Similar results were observed in quiescent cells upon serum stimulation (Figure 1B). The rapid decline of Cdk1 levels following the elimination of Cdk7 prevented us from analysing the overall level of phosphorylation of the corresponding Thr161 residue of Cdk1. The CAK complex can also activate the other interphase Cdks, Cdk4 and Cdk6 (Lolli and Johnson, 2005). Unfortunately, no phospho-specific antibodies for their T-loop threonine residues are available. Thus, we examined whether their expression levels and overall *in vitro* kinase activity was affected in MEFs lacking Cdk7. As illustrated in Figure 1A, *Cdk7*$^{mut/mut}$ MEFs expressed normal levels of Cdk4 and Cdk6. Moreover, the kinase activity of Cdk4 and Cdk6 immunoprecipitates derived from *Cdk7*$^{mut/mut}$ cells were significantly decreased, suggesting that CAK activity is compromised in cells lacking Cdk7 (Figure 1C). Similar results were obtained using Cdk2 immunoprecipitaes (Figure 1C). The kinase activity of Cdk1 could not be examined due to its low levels of expression in *Cdk7*$^{mut/mut}$ MEFs (Figure 1A and B).

Next, we interrogated whether Cdk7^{T170A}, a Cdk7 mutant that retains normal CAK function but $<$5% of the kinase activity towards the CTD of RNA pol II (Larochelle *et al*, 2001), was capable of rescuing proliferation of Cdk7 *null* cells. As illustrated in Figure 2, *Cdk7*$^{mut/mut}$ MEFs ectopically expressing the Cdk7^{T170A} mutant proliferated and formed colonies with efficiencies similar to those of cells ectopically expressing the wild-type Cdk7 protein. As a negative control, Cdk7^{K41A}, a kinase dead mutant, failed to induce both proliferation and colony formation (Figure 2A and B). These results support the notion that Cdk7 plays an essential role in cell proliferation by providing CAK activity whereas its CTD kinase activity is dispensable.

Cdk7 is required for T-loop phosphorylation of cell cycle Cdks

Next, we expressed phosphomimetic mutants of each of the cell cycle Cdks to determine which CAK substrate was responsible for cell proliferation. Neither Cdk4^{T174E} nor Cdk6^{T177E} mutants were able to convey proliferative properties to cells lacking Cdk7 (data not shown), suggesting that constitutive activation of these kinases is not sufficient to drive cell proliferation. We then performed a rescue assay using Cdk2^{T160E} or Cdk1^{T161E} phosphomimetic mutants. We observed that expression of Cdk2^{T160E} or Cdk1^{T161E}, but not their wild-type counterparts, partially restored proliferation and colony formation in Cdk7-deficient cells (Figure 2C and D). Colonies expressing these mutant proteins were analysed by Southern blotting to verify the absence of *Cdk7*^{lox} alleles (Supplementary Figure 2G). Yet, the proliferation rate and the number of colonies obtained with these Cdk1 and Cdk2 phosphomimetic mutants was lower than those observed with vectors expressing the wild-type Cdk7 protein (Figure 2C and D). Whether these differences are due to limited activity of the Cdk2^{T160E} or Cdk1^{T161E} mutants or to the fact that Cdk7 has additional functions that contribute to cell proliferation, remains to be determined.

Previous studies have shown that Cdk2 is neither essential for cell proliferation nor compensates for the absence of Cdk1, even when expressed from the *Cdk1* locus

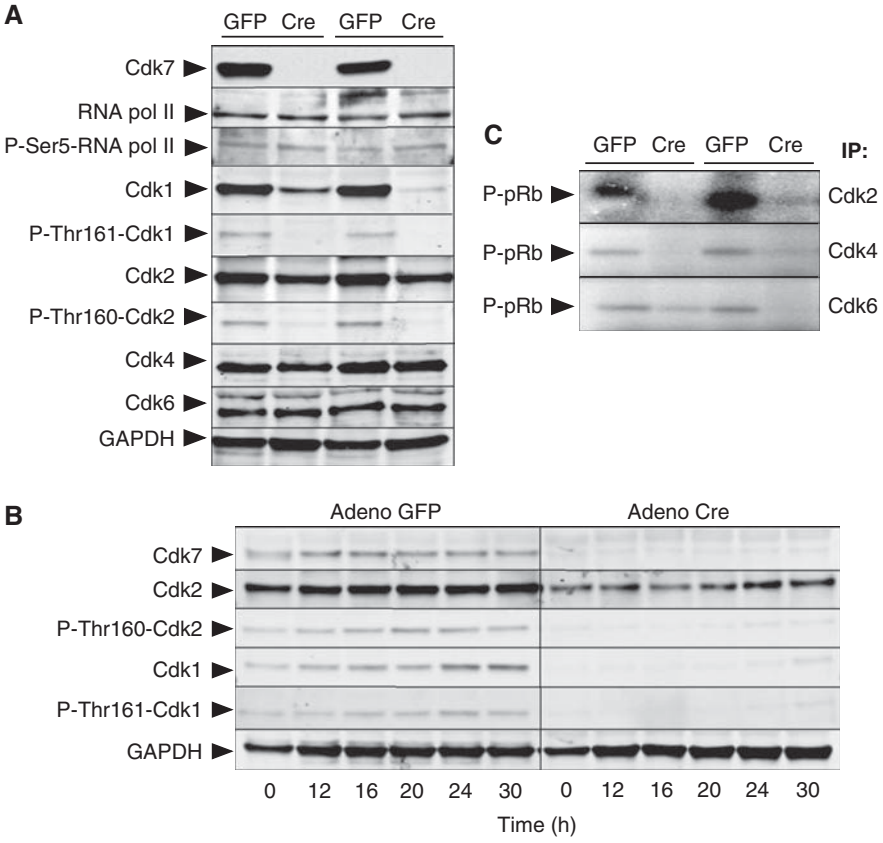

Figure 1 Deficient cell cycle Cdk activation in MEFs lacking Cdk7. (**A**) Immunoblot analysis of Cdk7, RNA pol II, P-Ser5-RNA pol II, Cdk1, P-Thr161-Cdk1, Cdk2, P-Thr160-Cdk2, Cdk4 and Cdk6 expression in extracts from *Cdk7*$^{lox/lox}$ MEFs infected with adenoviral particles expressing GFP or Cre recombinase. Results from two independent experiments are shown. GAPDH serves as a loading control. (**B**) Immunoblot analysis of Cdk7, Cdk2, P-Thr160-Cdk2, Cdk1 and P-Thr161-Cdk1 expression at the indicated time points after addition of serum to quiescent *Cdk7*$^{lox/lox}$ MEFs infected with adenoviral particles expressing GFP or Cre recombinase. GAPDH serves as a loading control. (**C**) *In vitro* kinase activity associated with Cdk2, Cdk4 and Cdk6 immunoprecipitates obtained from *Cdk7*$^{lox/lox}$ MEFs after infection with adenoviral particles expressing GFP or Cre recombinase. Recombinant pRb was used as substrate. Results from two independent experiments are shown. Figure source data can be found with the Supplementary data.

(Berthet *et al*, 2003; Ortega *et al*, 2003; Satyanarayana *et al*, 2008). Thus, we examined the mechanism by which the Cdk2^{T160E} mutant conferred proliferative properties to Cdk7-deficient cells. As shown in Figure 2G, expression of Cdk2^{T160E} in *Cdk7*$^{mut/mut}$ MEFs restored normal levels of Cdk1 protein that was properly phosphorylated in its Thr161 residue. These observations suggest that in the absence of Cdk7, Cdk2^{T160E} induces the synthesis of Cdk1 through inhibition of pRb and subsequent activation of the E2F-dependent transcriptional programme. Moreover, they also raised the possibility that Cdk2^{T160E} might activate Cdk1 by inducing phosphorylation in its critical Thr161 residue.

Restoration of E2F-dependent transcription rescues proliferation of Cdk7-defective cells

Microarray analysis revealed that, unlike housekeeping genes, the E2F-controlled programme (Bracken *et al*, 2004) was consistently downregulated (FDR 0.068) in *Cdk7*$^{mut/mut}$ MEFs (Supplementary Figure 2H). Downregulated genes included critical cell cycle regulators such as CycE1, CycA2, CycB1 and Cdk1. These observations were confirmed by western blotting (data not shown). These results suggest that reactivation of the E2F transcriptional programme by inactivation of the Rb family of proteins might alleviate the proliferative defects caused by elimination of Cdk7. To test this hypothesis, we expressed the T121 fragment of the SV40 large T antigen in *Cdk7*$^{mut/mut}$ MEFs. This polypeptide is known to inactivate the three members of the Rb family and improve the proliferation rate of cells lacking all interphase Cdks (Santamaría *et al*, 2007). As illustrated in Figure 2E and F, ectopic expression of T121 restored the proliferative properties of *Cdk7*$^{mut/mut}$ cells to the same level as the wild-type Cdk7 protein. Interestingly, these T121-expressing *Cdk7*$^{mut/mut}$ MEFs displayed normal levels of Cdk1 and Cdk2. Moreover, both kinases were properly phosphorylated in their activating T-loop Thr residues (Figure 2G). These observations indicate that cells have mechanisms other than Cdk7-mediated CAK activity to phosphorylate Cdk1 and Cdk2, providing that the Rb family of proteins has been inactivated.

Cdk7 deficiency causes early embryonic lethality

To characterize the impact of Cdk7 deficiency *in vivo*, we generated mice from ES cells carrying a *Cdk7*^{loxfrt} allele (Supplementary Figure 1). Heterozygous animals had normal lifespan and did not display obvious phenotypes. However, crosses between heterozygous animals failed to produce live

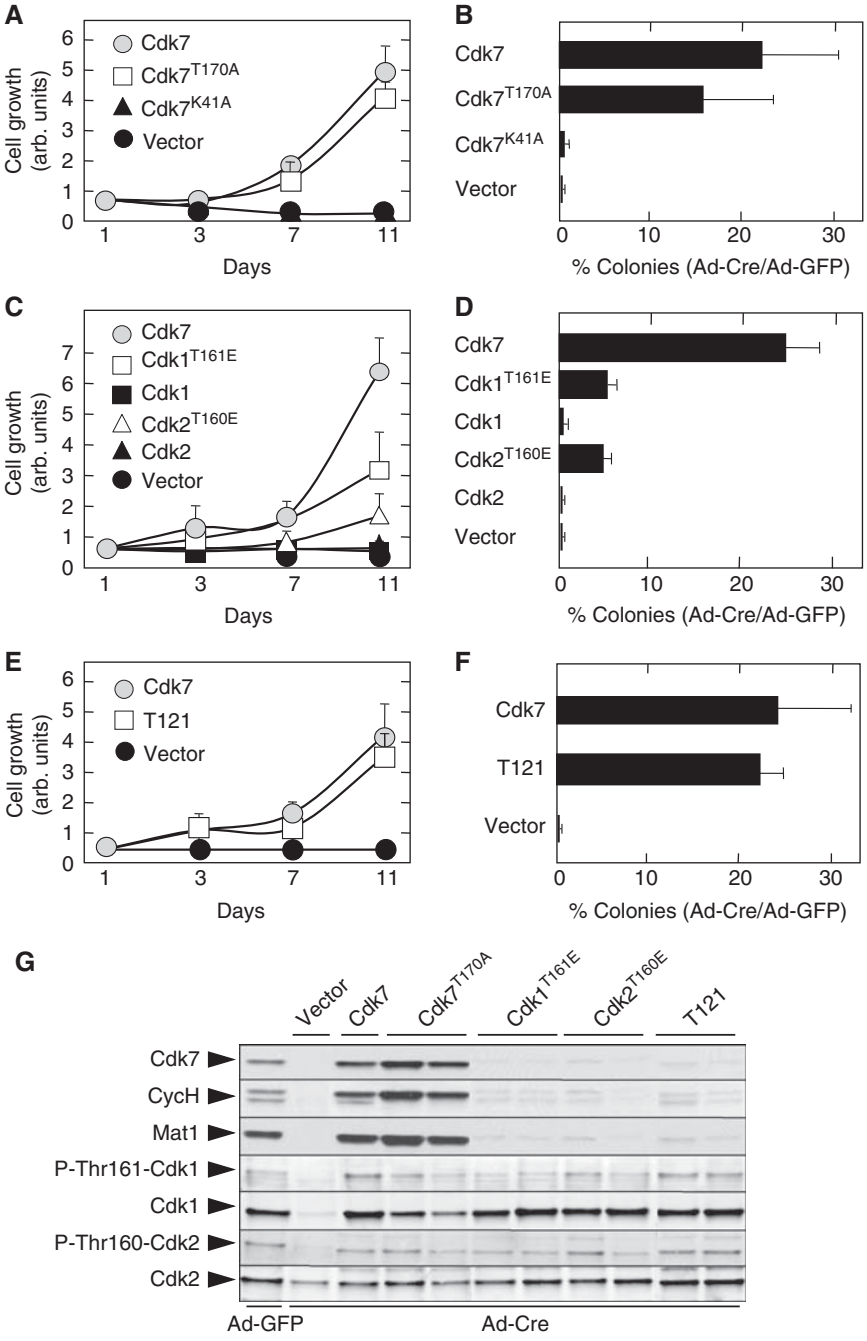

Figure 2 The CAK activity of Cdk7 is essential for cell proliferation. (**A**) Growth of immortalized *Cdk7*$^{lox/lox}$ MEFs infected with retroviral vectors expressing cDNAs encoding wild-type Cdk7 (grey circles), Cdk7^{T170A} (open squares), Cdk7^{K41A} (solid triangles) or control vector (solid circles) and subsequently infected with Ad-Cre to inactivate the *Cdk7*^{lox} alleles. (**B**) Percentage of colonies observed in *Cdk7*$^{lox/lox}$ MEFs infected with retroviral vectors expressing cDNAs encoding wild-type Cdk7, mutant Cdk7^{T170A}, mutant Cdk7^{K41A} or with control vector and subsequently infected with Ad-Cre, normalized to those observed in parallel cultures infected with control Ad-GFP. Data shown as mean ± s.d., $n = 3$. (**C**) Growth of immortalized *Cdk7*$^{lox/lox}$ MEFs infected with retroviral vectors expressing cDNAs encoding wild-type Cdk7 (grey circles), phosphomimetic Cdk1^{T161E} mutant (open squares), wild-type Cdk1 (solid squares), phosphomimetic Cdk2^{T160E} mutant (open triangles), wild-type Cdk2 (solid triangles) or with control vector (solid circles) and subsequently infected with Ad-Cre to inactivate the *Cdk7*^{lox} alleles. (**D**) Percentage of colonies observed in *Cdk7*$^{lox/lox}$ MEFs infected with retroviral vectors expressing cDNAs encoding wild-type Cdk7, phosphomimetic Cdk1^{T161E} and Cdk2^{T160E} mutant proteins, wild-type Cdk1 or Cdk2 proteins or with control vector and subsequently infected with Ad-Cre, normalized to those observed in parallel cultures infected with Ad-GFP. Data shown as mean ± s.d., $n = 3$. (**E**) Growth of immortalized *Cdk7*$^{lox/lox}$ MEFs infected with retroviral vectors expressing a cDNA encoding wild-type Cdk7 (grey circles), the T121 fragment of the SV40 large T antigen (open squares) or with control vector (solid circles) and subsequently infected with Ad-Cre to inactivate the *Cdk7*^{lox} alleles. (**F**) Percentage of colonies observed in *Cdk7*$^{lox/lox}$ MEFs infected with retroviral vectors expressing a cDNA encoding wild-type Cdk7, the T121 fragment of the SV40 large T antigen or with control vector and subsequently infected with Ad-Cre, normalized to those observed in parallel cultures infected with Ad-GFP. Data shown as mean ± s.d., $n = 3$. (**G**) Immunoblot analysis of Cdk7, CycH, Mat1, Cdk1, P-Thr161-Cdk1, Cdk1, P-Thr160-Cdk2 and Cdk2 expression in representative colonies of immortalized *Cdk7*$^{lox/lox}$ MEFs infected with retroviral vectors expressing cDNAs encoding wild-type Cdk7, mutant Cdk7^{T170A}, phosphomimetic Cdk1^{T161E} and Cdk2^{T160E} mutants, the T121 fragment of the SV40 large T antigen or with control vector and subsequently infected with Ad-Cre to inactivate the *Cdk7*^{lox} alleles or with control Ad-GFP. Figure source data can be found with the Supplementary data.

Cdk7$^{loxfrt/loxfrt}$ offspring as well as E13.5 and E9.5 embryos, thus suggesting that *Cdk7*^{loxfrt} alleles failed to express normal levels of Cdk7 (see below). Analysis of E5.5 embryos derived from these crosses revealed deciduas with a high percentage of apoptotic cells within the embryonic body that were negative for Cdk7 immunostaining (Supplementary Figure 3A), thus suggesting that homozygous *Cdk7*$^{loxfrt/loxfrt}$ embryos died at peri-implantation stages. Interestingly, E2.5 as well as E3.5 *Cdk7*$^{loxfrt/loxfrt}$ embryos (blastocyst stage) were obtained with Mendelian ratios. As the E2.5 mutant embryos did not express detectable levels of Cdk7 (Figure 3A), the apparently normal development of *Cdk7*$^{loxfrt/loxfrt}$ blastocysts is unlikely to be due to contribution by the maternal Cdk7 protein.

To study the defects responsible for the death of *Cdk7*$^{loxfrt/loxfrt}$ embryos, we isolated E2.5 embryos and maintained them under *in vitro* culture conditions. One day later, the resulting E3.5 *Cdk7*$^{loxfrt/loxfrt}$ blastocysts were indistinguishable from the heterozygous and wild-type littermates, including normal levels of expression of Nanog, an inner cell mass (ICM) marker (Figure 3B), thus indicating that early embryo cells can differentiate into ICM lineages in the absence of Cdk7. However, at E4.5, *Cdk7*$^{loxfrt/loxfrt}$ embryos showed conspicuous staining of the apoptotic marker-activated Caspase 3A within the ICM (Figure 3C), leading to the disappearance of ICM cells 2 days later in hatching embryos (Figure 3D). At this time (E6.5–E7.5), visual inspection of *Cdk7*$^{loxfrt/loxfrt}$ embryos revealed the presence of trophoblasts. However, their nuclei appeared smaller (3–4-fold) than those of trophoblasts present in control embryos (Supplementary Figure 3B and C). These observations suggest that *Cdk7*$^{loxfrt/loxfrt}$ embryos die during peri-implantation stages due to apoptotic death of ICM cells. Furthermore, the smaller size of the nuclei of *Cdk7*$^{loxfrt/loxfrt}$ trophoblasts suggests additional defects in the trophoectodermal lineage, most likely due to limited endoreplicative cycles.

Cdk7 is required for skin development

Next, we analysed the role of Cdk7 during skin development. To this end, we generated a conditional *Cdk7*$^{lox/lox}$ mice by crossing *Cdk7*$^{loxfrt/loxfrt}$ animals to a Flpase-expressing strain, as described in Materials and methods. The resulting *Cdk7*$^{lox/lox}$ animals were subsequently crossed to K5-Cre, a transgenic strain that selectively expresses the Cre recombinase within the basal layer of the epidermis (Tarutani *et al,* 1997). *Cdk7*$^{lox/lox}$; K5-Cre$^{+/T}$ compound mice were born with Mendelian ratios. However, they displayed small size, widespread lack of hair, scaly skin and died soon thereafter, between postnatal days 1 and 4 (P1–P4) (Figure 4A). Immunohistochemical analysis of the skin of these mice revealed mosaic elimination of Cdk7, with patches of epidermis showing positive staining interspersed with regions lacking Cdk7 expression (Figure 4B). In agreement with *in vitro* studies, phosphorylation in the Ser5 residue of the CTD of RNA pol II was unaffected in these cells (Figure 4B). Likewise, cells lacking Cdk7 displayed pRb hypophosphorylation and were negative for P-Thr160-Cdk2, suggesting that Cdk7 is also required for the activation of Cdk2 *in vivo*.

Histopathological analysis of skin samples of *Cdk7*$^{lox/lox}$;K5-Cre$^{+/T}$ mice revealed a complex phenotype. The epidermis of these animals showed scattered hyperplastic and hypoplastic regions (Figure 4C). The latter were devoid of Cdk7 staining and contained non-proliferating cells as indicated by the absence of PCNA staining, a marker of cell proliferation (Figure 4D). On the

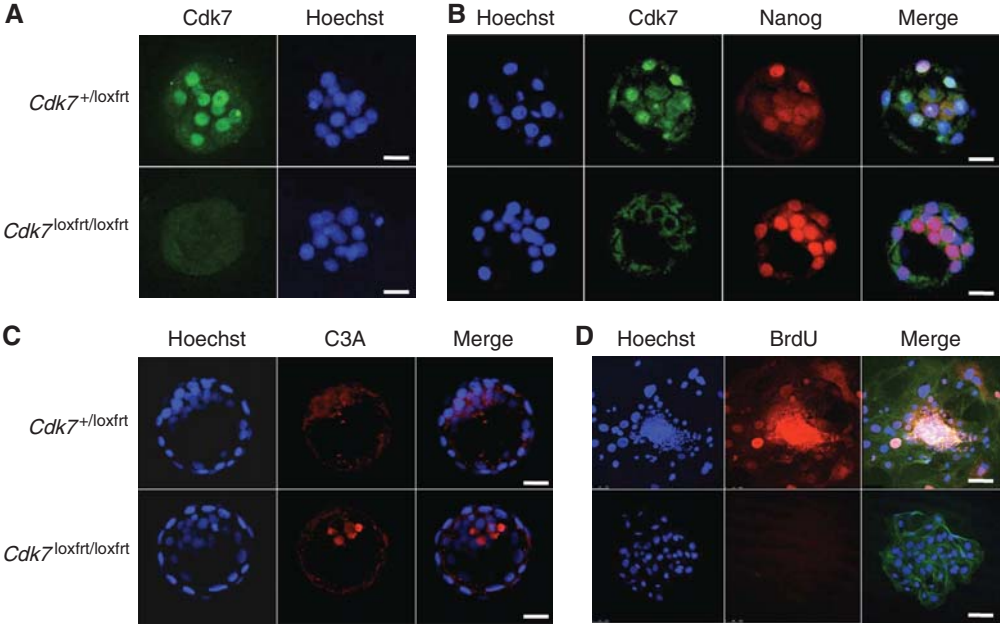

Figure 3 *Cdk7* germ line deficiency results in an early embryonic lethality. (**A**) Embryos of the indicated genotypes were isolated at E2.5 and analysed for Cdk7 expression by immunofluorescence (green). Nuclei were stained with Hoechst 33342 (blue). Bar, 25 μm. (**B**) Embryos of the indicated genotypes were isolated at E2.5, cultured *in vitro* and analysed by immunofluorescence at E3.5. Co-staining for Cdk7 (green) and Nanog (red) is shown. Nuclei were stained with Hoechst 33342 (blue). Bar, 25 μm. (**C**) Embryos of the indicated genotypes were isolated at E2.5 and cultured *in vitro* for 2 days (E4.5 stage). Active Caspase 3 was detected by immunofluorescence (red). Nuclei were stained with Hoechst 33342 (blue). Bar, 25 μm. (**D**) Embryos of the indicated genotypes were isolated at E2.5 and cultured *in vitro* for 5 days (E7.5 stage). BrdU incorporation was assessed by immunofluorescence (red). Nuclei were stained with Hoechst 33342 (blue). Actin filaments were stained with Phalloidin (green). Bar, 100 μm.

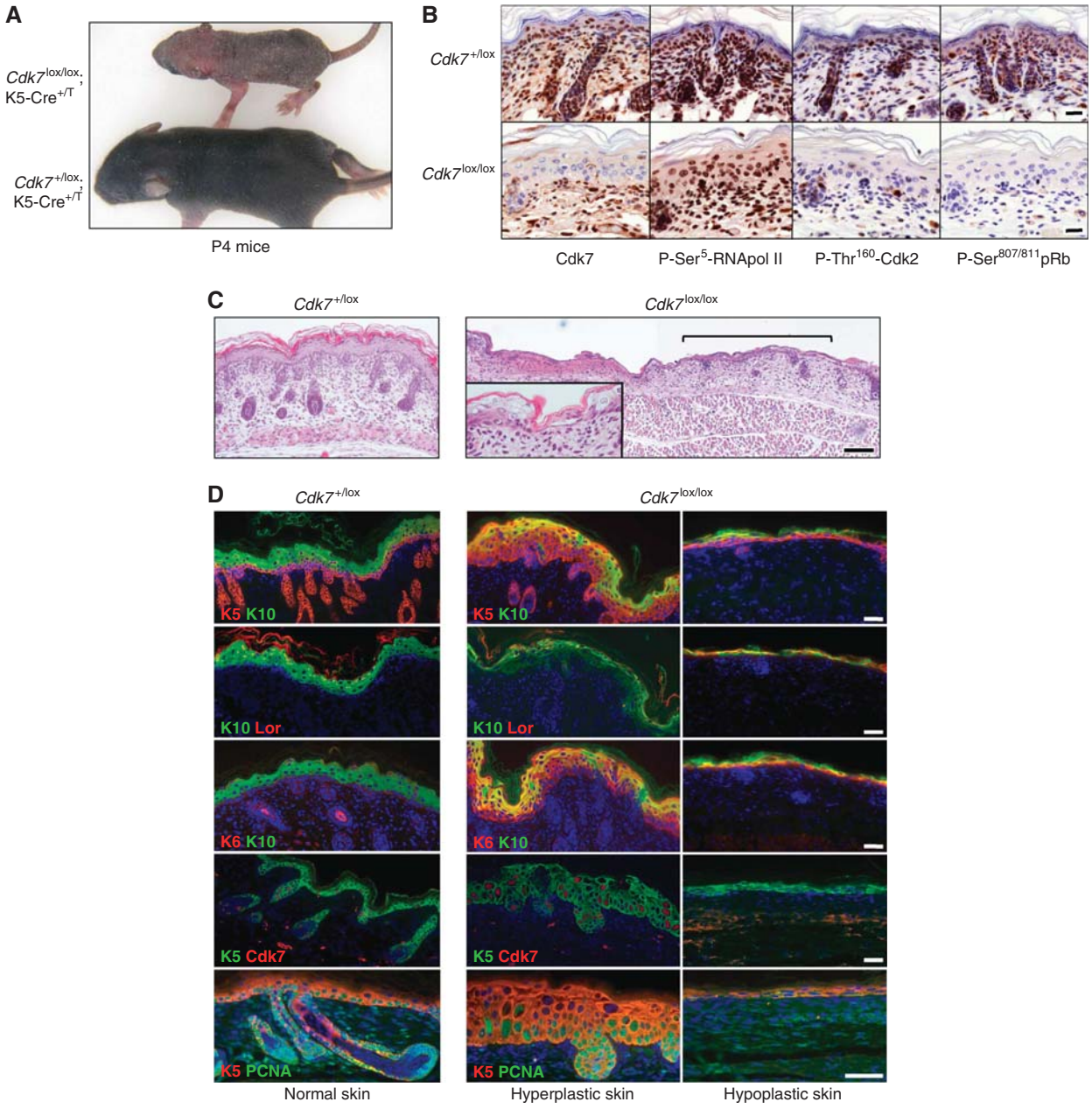

Figure 4 Cdk7 is required for skin development. (**A**) Overall appearance of *Cdk7*$^{+/lox}$;K5-Cre$^{+/T}$ and *Cdk7*$^{lox/lox}$;K5-Cre$^{+/T}$ P4 mice. **(B)** Immunohistochemical staining of representative skin areas obtained from *Cdk7*$^{+/lox}$;K5-Cre$^{+/T}$ and *Cdk7*$^{lox/lox}$;K5-Cre$^{+/T}$ P4 mice using antibodies against Cdk7, P-Ser5-RNA pol II, P-Thr160-Cdk2 and P- Ser807/811-pRb. Bar, 20 μm. (**C**) H&E staining of skin sections of *Cdk7*$^{+/lox}$;K5-Cre$^{+/T}$ and *Cdk7*$^{lox/lox}$;K5-Cre$^{+/T}$ P4 mice. Bracket indicates a hypoplastic area in the skin of a *Cdk7*$^{lox/lox}$;K5-Cre$^{+/T}$ P4 mouse flanked by hyperplastic regions. Inset shows a magnified image of hypoplastic skin flanked by hyperplastic areas of a *Cdk7*$^{lox/lox}$;K5-Cre$^{+/T}$ P4 mouse. Bar, 100 μm. (**D**) Immunofluorescence analysis of normal skin sections of *Cdk7*$^{+/lox}$;K5-Cre$^{+/T}$ P4 mice (left) and of hyperplastic (middle) and hypoplastic (right) skin areas of *Cdk7*$^{lox/lox}$;K5-Cre$^{+/T}$ P4 mice using antibodies raised against keratin K5, keratin K6, keratin K10, Cdk7, Loricrin (Lor) and PCNA. Antibodies are labelled in red or green colour according to the immunofluorescence they displayed in the corresponding sections. Bar, 50 μm.

contrary, cells within the hyperplastic regions were positive for Cdk7 expression, indicating that recombination of *Cdk7*^{lox} alleles was not complete. Most of these Cdk7-expressing cells were also positive for PCNA, indicating that they were actively proliferating.

The hypoplastic regions displayed delayed development, thinning of the suprabasal layers as determined by keratin K10 staining and a severe reduction in the number of hair follicles (Figure 4D). Furthermore, they showed an altered differentiation pattern illustrated by the misexpression of keratin K6 in both the basal and suprabasal layers of the interfollicular epidermis (Figure 4C and D). Interestingly, keratin K6 was also misexpressed throughout the epidermis in hyperplastic areas, suggesting that these regions also experienced an altered homeostasis. Finally, hyperplastic regions were additionally characterized by an expansion of keratin K5-expressing cells to the suprabasal layers and by a concomitant disorganization of these layers as determined by

the expression pattern of keratin K10 and loricrin (Figure 4D). Altogether, these observations suggest that ablation of Cdk7 in the epidermis results in the cessation of cell proliferation leading to hypoplastic skin. As a consequence, neighbouring areas that retained Cdk7 expression due to mosaic recombination of the $Cdk7^{lox}$ alleles underwent an aberrant hyperproliferative response, most likely a homeostatic attempt to compensate the lack of proliferation within the nearby hypoplastic patches.

Deletion of Cdk7 in adult mice

These results prompted us to investigate the consequences of widespread elimination of Cdk7 in adult tissues. To this end, $Cdk7^{+/lox}$ mice were crossed to Ub-CreERT2$^{+/T}$ animals, a transgenic strain that expresses the tamoxifen-inducible CreERT2 recombinase under the control of the human ubiquitin C promoter (Ruzankina *et al*, 2007). $Cdk7^{lox/lox}$;Ub-CreERT2$^{+/T}$ mice were exposed at weaning to a tamoxifen-containing diet to ablate the conditional *Cdk7* alleles. Four-month-old $Cdk7^{lox/lox}$;Ub-CreERT2$^{+/T}$ animals were phenotypically normal in spite of lacking Cdk7 expression in most (>90%) cells within low proliferating tissues such as liver, kidney or cerebellum (Figure 5A). These mice exhibited normal physiological levels of several key biochemical parameters in plasma including glucose, amylase, bilirubin, albumin and alanine aminotransferase (Supplementary Figure 4). Other parameters such as total protein, globulin, calcium, phosphate and ureic nitrogen also remained at normal levels in $Cdk7^{lox/lox}$;Ub-CreERT2$^{+/T}$ animals (Supplementary Figure 4). Similar results were obtained when we analysed the endocrine pancreas. $Cdk7^{lox/lox}$;Ub-CreERT2$^{+/T}$ mice had the same pattern of insulin and glucagon-expressing cells as control $Cdk7^{+/lox}$;Ub-CreERT2$^{+/T}$ animals, in spite of the fact that most of these cells lacked Cdk7 expression (Figure 5B). As illustrated above in newborn skin (Figure 4B), the levels of phosphorylated Ser5 residues in RNA pol II of $Cdk7^{lox/lox}$;Ub-CreERT2$^{+/T}$ mice were unaffected by the loss of Cdk7 expression in all tissues examined (Figure 5A). Phosphorylation levels of Cdk1^{T161} and Cdk2^{T160} could not be determined as these proteins are not expressed in the large majority of cells (>98%) in these non-proliferating tissues (data not shown).

Loss of Cdk7 expression in actively dividing tissues results in accelerated aging

$Cdk7^{lox/lox}$;Ub-CreERT2$^{+/T}$ animals retained Cdk7 expression in their proliferating tissues such as the intestine and skin, even when exposed to the tamoxifen diet for 7 months (Figure 6A). An observation that might explain the relatively long survival of these mice (Supplementary Figure 5B). Expression of Cdk7 in these highly proliferating tissues was not due to impaired recombination of their $Cdk7^{lox}$ alleles as they were efficiently ablated in heterozygous $Cdk7^{+/lox}$;Ub-CreERT2$^{+/T}$ mice exposed to the same diet (Supplementary Figure 5A). To explain these observations, we hypothesized that the presence of Cdk7 in these proliferating tissues might be due to an active process of cell renewal sustained by a pool of adult stem cells that had retained Cdk7 expression. If so, such a continuous demand on adult stem cells should result in their premature exhaustion leading to the appearance of aging-like phenotypes (Krishnamurthy and Sharpless, 2007). Indeed, visual inspection of 8-month-old

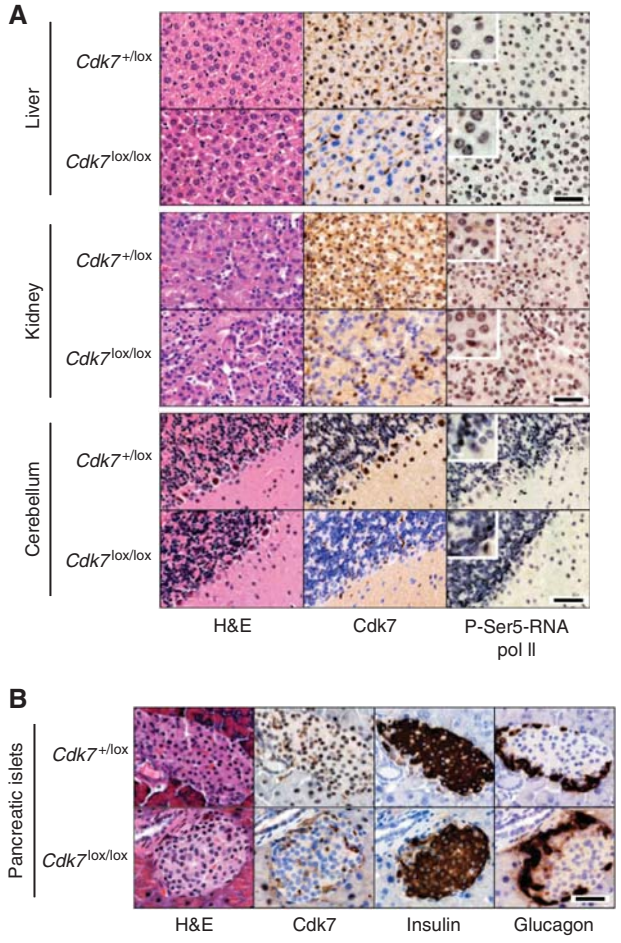

Figure 5 Lack of physiological defects upon Cdk7 elimination in young mice. (**A**) H&E and immunochemical staining of sections obtained from liver (top), kidney (middle) and cerebellum (bottom) of 4-month-old $Cdk7^{+/lox}$;Ub-CreERT2$^{+/T}$ and $Cdk7^{lox/lox}$;Ub-CreERT2$^{+/T}$ littermates exposed to a tamoxifen diet for 3 months. Immunostaining was carried out with antibodies elicited against Cdk7 and against P-Ser5-RNA pol II. Insets show magnified images of representative areas. Bar, 50 μm. (**B**) H&E and immunochemical staining of consecutive sections of pancreatic islets obtained from 4-month-old $Cdk7^{+/lox}$;Ub-CreERT2$^{+/T}$ and $Cdk7^{lox/lox}$;Ub-CreERT2$^{+/T}$ littermates exposed to a tamoxifen diet for 3 months. Immunostaining was carried out with antibodies elicited against Cdk7, insulin and glucagon. Bar, 50 μm.

$Cdk7^{lox/lox}$;Ub-CreERT2$^{+/T}$ mice exposed to a tamoxifen diet as weaning revealed a variety of age-related phenotypes not present in $Cdk7^{+/lox}$;Ub-CreERT2$^{+/T}$ control littermates (Figure 6B). These phenotypes included a significant body weight loss, with $Cdk7^{lox/lox}$;Ub-Cre$^{+/T}$ females weighing an average of 30% less than the control animals ($14.36 \pm 2.63\,g$ versus $20.27 \pm 1.28\,g$; $n = 8$; $P < 0.001$), diffuse alopecia, pervasive hair-greying and kyphosis (Figure 6B).

Further characterization of these mice revealed additional age-related phenotypes affecting bones, hematopoietic and intestinal tissues as well as skin. Densitometric analysis of the femurs of $Cdk7^{lox/lox}$;Ub-CreERT2$^{+/T}$ animals revealed that their mineral content was significantly reduced compared with that of control littermates ($0.33 \pm 0.003\,g$ versus $0.41 \pm 0.021\,g$; $n = 4$; $P < 0.001$). Furthermore, computed tomography (CT) scanning revealed that the cortical cross section (0.40 mm ± 0.009 versus 0.54 mm ± 0.03; $n = 4$;

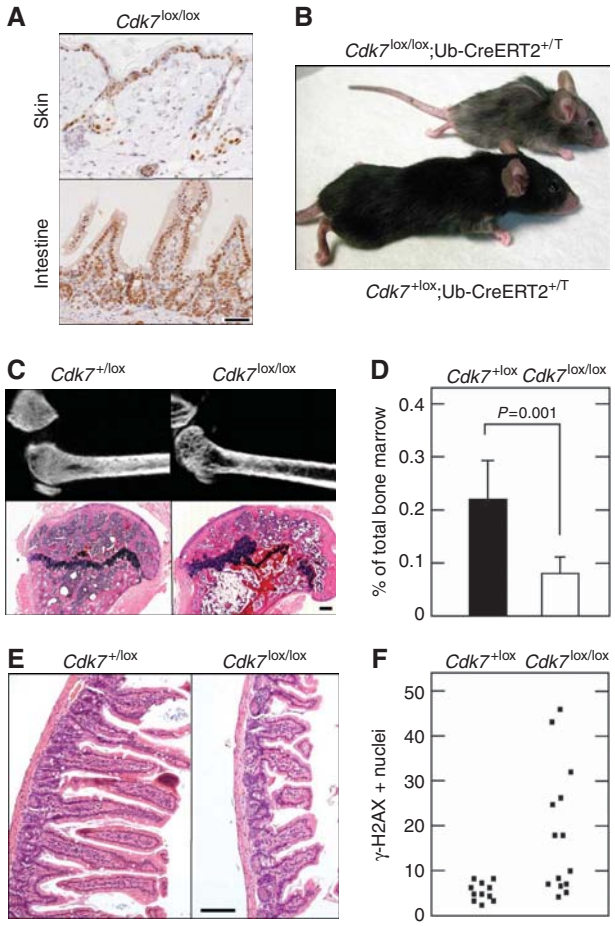

Figure 6 Widespread elimination of Cdk7 expression in adult mice results in premature aging. (**A**) Immunochemical staining of skin (top) and the small intestine (bottom) from 8-month-old $Cdk7^{lox/lox}$;Ub-CreERT2$^{+/T}$ animals exposed to a tamoxifen diet for 7 months. Bar, 50 μm. (**B**) Overall appearance of 8-month-old $Cdk7^{+/lox}$;Ub-CreERT2$^{+/T}$ mice and $Cdk7^{lox/lox}$;Ub-CreERT2$^{+/T}$ littermates exposed to a tamoxifen diet for 7 months. (**C**) Micro-CT analysis of femurs (top) and H&E staining of femur sections (bottom) obtained from 8-month-old $Cdk7^{+/lox}$;Ub-CreERT2$^{+/T}$ and $Cdk7^{lox/lox}$;Ub-CreERT2$^{+/T}$ littermates exposed to a tamoxifen diet for 7 months. Bar, 100 μm. (**D**) Quantification of hematopoietic Lin$^-$Sca-1$^+$c-Kit^{hi} progenitors in the bone marrow of $Cdk7^{+/lox}$;Ub-CreERT2$^{+/T}$ (solid bar, $n=5$) and $Cdk7^{lox/lox}$;Ub-CreERT2$^{+/T}$ (open bar, $n=7$) littermates exposed to a tamoxifen diet for 7 months. Data shown as mean ± s.d. A student's *t*-test was used to calculate statistical significance. (**E**) H&E staining of small intestine sections of $Cdk7^{+/lox}$;Ub-CreERT2$^{+/T}$ and $Cdk7^{lox/lox}$;Ub-CreERT2$^{+/T}$ littermates exposed to a tamoxifen diet for 7 months. Bar, 100 μm. (**F**) Number of cells showing positive nuclei for γ-H2AX phosphorylation in liver sections of $Cdk7^{+/lox}$;Ub-CreERT2$^{+/T}$ and $Cdk7^{lox/lox}$;Ub-CreERT2$^{+/T}$ littermates exposed to a tamoxifen diet for 7 months. Each dot represents the total number of nuclei with positive staining in 20 microscope fields. Positive cells were detected by immunohistochemistry.

$P<0.001$) and the trabecular bone content were also reduced in the $Cdk7^{lox/lox}$;Ub-CreERT2$^{+/T}$ cohort (Figure 6C). In addition, some of the bone marrow had been replaced by adipose tissues (Moerman *et al*, 2004).

Eight-month-old $Cdk7^{lox/lox}$;Ub-CreERT2$^{+/T}$ mice exposed to tamoxifen diet also had reduced levels of Lin$^-$Sca-1$^+$c-Kit^{hi} hematopoietic progenitors (Figure 6D), hypoplastic crypts and villi in the small intestine (Figure 6E) and increased the number of hepatocytes with positive staining for phosphorylated histone γ-H2AX (Figure 6F, Ruzankina *et al*, 2007; Matheu *et al*, 2007). All $Cdk7^{lox/lox}$;Ub-CreERT2$^{+/T}$ mice examined ($n=8$) a displayed progressive nephropathy and severe medullary calcification, two age-related defects that were only marginally present in some $Cdk7^{+/lox}$;Ub-CreERT2$^{+/T}$ control littermates (Supplementary Figure 5C, Chuttani and Gilchrest, 1995; Haines *et al*, 2001). Finally, skin tissue also showed phenotypic marks associated with premature aging, including reduced dermal thickness, loss of the subcutaneous adipose layer and transformation of follicular epithelium into sebaceous glands (Figure 7A and B). Interestingly, most of the physiological parameters of these 8-month-old $Cdk7^{lox/lox}$;Ub-CreERT2$^{+/T}$ mice, including key biochemical factors in plasma as well as levels of globulin, calcium, phosphate and ureic nitrogen, remained mostly unaffected (Supplementary Figure 4).

Stem cell exhaustion in Cdk7 depleted skin

As reasoned above, these ageing phenotypes are likely to result from the exhaustion of stem cell compartments that have retained Cdk7 expression. As illustrated in Figure 7A, the bulge region of the hair follicles of $Cdk7^{lox/lox}$;Ub-CreERT2$^{+/T}$ mice were almost deprived of epithelial stem cells characterized by coexpression of keratin K15 and CD34 (Lyle *et al*, 1998; Blanpain *et al*, 2004). Progressive shortening of telomeres is a hallmark associated with persistent cell division that parallels a decline in stem cell functionality (Flores *et al*, 2008; Flores and Blasco, 2010). Thus, telomere length may serve as a marker to determine whether the reduced number of stem cells in the skin of $Cdk7^{lox/lox}$;Ub-CreERT2$^{+/T}$ mice arose as a consequence of stem cell exhaustion. As shown in Figure 7C, quantitative telomere Q-FISH analysis revealed a significant reduction in the average telomere length in the skin cells of $Cdk7^{lox/lox}$;Ub-CreERT2$^{+/T}$ mice compared with those of $Cdk7^{+/lox}$;Ub-CreERT2$^{+/T}$ littermate controls. Furthermore, the overall distribution of telomere length in $Cdk7^{lox/lox}$;Ub-CreERT2$^{+/T}$ skin was shifted towards undersized values with a substantial increase in the percentage of short telomeres (Figure 7D and E). This difference is maximized when the skin telomere length is normalized to that of a non-proliferative tissue (Figure 7F), thus arguing that indeed telomere shortening occurred as a consequence of increased proliferative demand and not as a cell autonomous defect associated to Cdk7 elimination. Notably, the increased frequency of short telomeres, rather than the mean telomere length, is particularly determinant for telomere dysfunction and correlates with aging phenotypes (Hemann *et al*, 2001; Canela *et al*, 2009). Altogether, these observations indicate that skin cells of $Cdk7^{lox/lox}$;Ub-CreERT2$^{+/T}$ mice have endured an extended proliferative period, most likely to compensate for those cells that lost their proliferative capacity due to inactivation of their $Cdk7^{lox}$ alleles.

Discussion

In this study, we have provided genetic evidence indicating that Cdk7, the catalytic subunit of the trimeric CAK complex, is essential for cell proliferation. Indeed, Cdk7 is essential for activation of the cell cycle through phosphorylation of key threonine residues in the T-loops of the Cdks. In contrast,

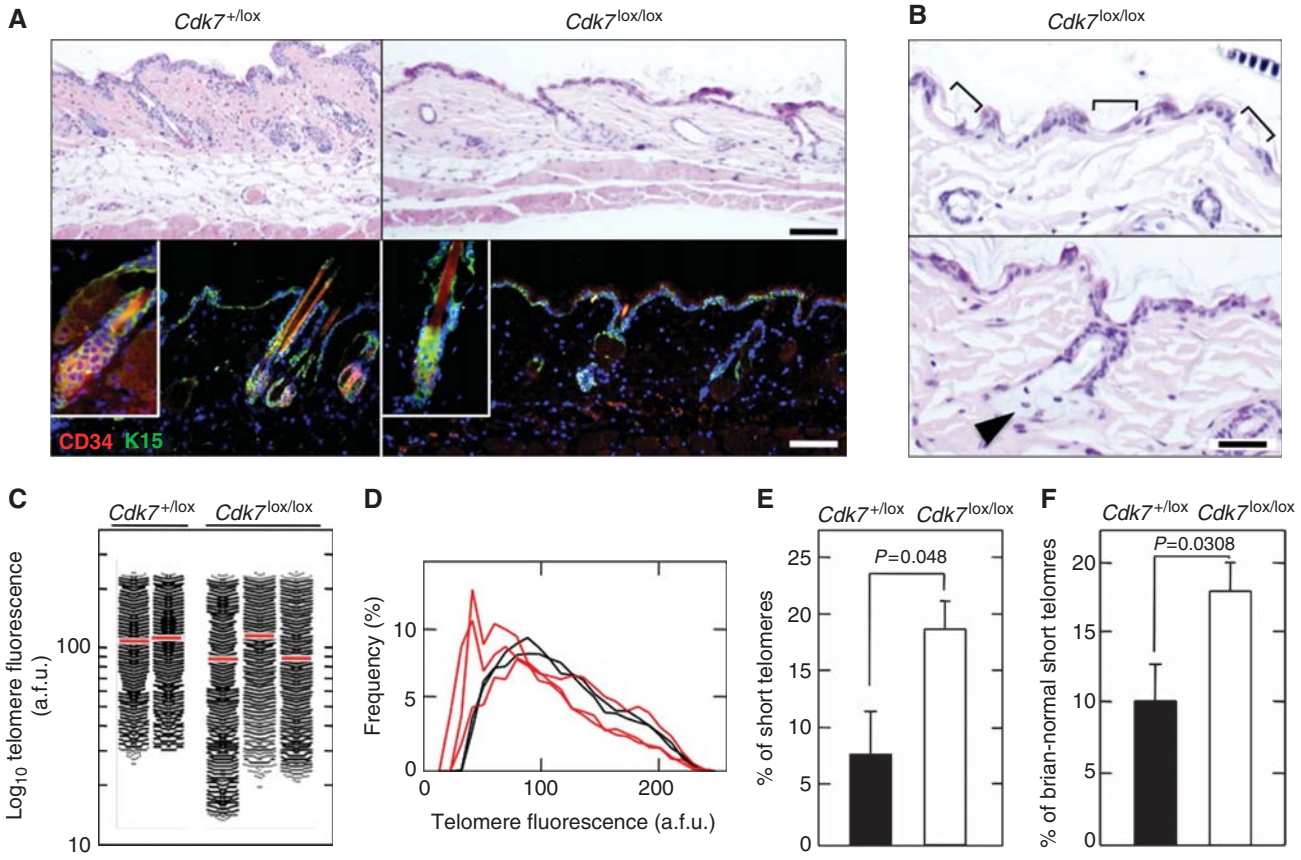

Figure 7 Loss of Cdk7 in the epidermis causes stem cell depletion and telomere shortening. (**A**) H&E (top) and immunuofluorescence (bottom) staining using antibodies against CD34 and keratin K15 of representative skin areas from 8-month-old *Cdk7*$^{+/lox}$;Ub-CreERT2$^{+/T}$ and *Cdk7*$^{lox/lox}$;Ub-CreERT2$^{+/T}$ mice exposed to a tamoxifen diet for 7 months. Antibodies are labelled in red or green colour according to the immunofluorescence they displayed in the corresponding sections. Insets show magnified images to illustrate that the stem cell pool of the hair bulge is mostly exhausted in *Cdk7*$^{lox/lox}$;Ub-CreERT2$^{+/T}$ mice. Bar, 100 μm. (**B**) Magnified images of skin areas of *Cdk7*$^{lox/lox}$;Ub-CreERT2$^{+/T}$ mice to illustrate extreme epidermal thinning (brackets) (top) and conversion of hair follicles into adipose tissue (arrowhead) (bottom). Bar, 50 μm. (**C**) Telomere Q-FISH analysis of skin sections of 8-month-old *Cdk7*$^{+/lox}$;Ub-CreERT2$^{+/T}$ and *Cdk7*$^{lox/lox}$;Ub-CreERT2$^{+/T}$ mice exposed to a tamoxifen diet for 7 months. Red bars indicate average telomere fluorescence intensity. a.f.u., arbitrary fluorescence units. (**D**) Q-FISH histograms showing telomere fluorescence frequencies of data shown in **C** for *Cdk7*$^{+/lox}$;Ub-CreERT2$^{+/T}$ (black) and *Cdk7*$^{lox/lox}$;Ub-CreERT2$^{+/T}$ (red) mice. (**E**) Percentage of short telomeres (intensity ⩽10th percentile) in the skin of *Cdk7*$^{+/lox}$;Ub-CreERT2$^{+/T}$ (solid bar; $n=5$) and *Cdk7*$^{lox/lox}$;Ub-CreERT2$^{+/T}$ (open bar; $n=6$) littermates. Data shown as mean ± s.d. A student's *t*-test was used to calculate statistical significance. (**F**) Percentage of short telomeres (intensity ⩽10th percentile) in skin upon normalization to their respective brain values from *Cdk7*$^{+/lox}$;Ub-CreERT2$^{+/T}$ (solid bar; $n=4$) and *Cdk7*$^{lox/lox}$;Ub-CreERT2$^{+/T}$ (open bar; $n=4$) littermates. Data shown as mean ± s.d. A student's *t*-test was used to calculate statistical significance.

Cdk7 is completely dispensable for phosphorylation of the critical Ser5 residue located in the CTD of RNA pol II and for regulating overall transcription. These results are reminiscent of those previously obtained for Mat1, one of the regulatory subunits of the CAK complex (Rossi *et al*, 2001; Korsisaari *et al*, 2002), and with previous findings in lower organisms in which RNA pol II-mediated transcription is only marginally affected upon elimination of Cdk7 activity (Larochelle *et al*, 1998; Lee *et al*, 2005; Wallenfang and Seydoux, 2002).

Genetic inactivation of *Cdk7*^{lox} alleles led to a loss of T-loop phosphorylation, damped Cdk activity and cell cycle arrest. Indeed, the Cdk1 and Cdk2 T-loop phosphomimetic mutants, Cdk1^{T161E} and Cdk2^{T160E}, partially restored proliferation in cells deprived of Cdk7. These observations suggest that the inability of Cdk7-defficient cells to proliferate could be explained by the lack of Cdk1 activity. However, the mechanism by which Cdk2^{T160E} induces cell proliferation in the absence of Cdk7 is less clear as previous genetic studies have demonstrated that Cdk2 is completely dispensable for cell division (Berthet *et al*, 2003; Ortega *et al*, 2003). The presence of active P-Thr161-Cdk1 in Cdk2^{T160E}-expressing *Cdk7*$^{mut/mut}$ cells suggests that Cdk2^{T160E}, either directly or indirectly, induces phosphorylation of the T-loop of Cdk1. Whether Cdk2 plays a role in the activation of Cdk1 in normal cells expressing Cdk7 remains to be determined.

Loss of Cdk7 also contributes to cell cycle arrest by decreasing the E2F-controlled transcription levels, including genes essential for cell cycle progression such as CycA2 and Cdk1. In view of the lack of effect of Cdk7 on RNA pol II-driven global transcription, the decreased levels of expression of E2F-controlled genes is most likely a consequence of the decreased Cdk activity and subsequent hypophosphorylation of the pocket proteins. These observations are reminiscent of those observed in *S. pombe* where loss of Mcs6, the Cdk7 orthologue, showed a modest effect on global gene expression while selectively affected the expression of a cell-division cluster (Lee *et al*, 2005). Indeed, inactivation of the three Rb family members by ectopic expression of the SV40 T121 fragment

restored the proliferation of Cdk7-deficient MEFs. Interestingly, these T121-expressing *Cdk7*$^{mut/mut}$ cells displayed normal levels of P-Thr161-Cdk1 and P-Thr160-Cdk2.

Our results cannot rule out a requirement of Cdk7 for transcription of E2F-controlled genes. Yet, we favour the concept that E2F-mediated transcription is only affected indirectly upon Cdk7 ablation due to an overall decrease in Cdk activity and hypophosphorylation of pRb. The lack of effect on RNA pol II-mediated transcription might simply reflect the compensation of Cdk7 function by other kinases. Indeed, several proteins, including the closely related Cdk9, have been reported to phosphorylate Ser5 in the CTD of RNA pol II (Palancade and Bensaude, 2003). Furthermore, inhibition of Cdk7 and Cdk9 is concomitantly required to eliminate Ser5 phosphorylation of RNA pol II (Ni *et al*, 2004). In fact, activation of Cdk9 does not rely on Cdk7 and therefore would remain active following CAK inhibition (Kim and Sharp, 2001).

Embryos lacking Cdk7 developed to peri-implantation stages before undergoing massive apoptosis. These observations are reminiscent of those obtained upon ablation of the Mat1 regulatory subunit (Rossi *et al*, 2001). However, Cdk7 mutant embryos do not require expression of the maternal Cdk7 protein. *In vitro*, these embryos also progressed to the blastocyst stage, but at E6.5 their ICM cells underwent apoptotic death. As Cdk1 activity is essential during the first cell divisions (Santamaría *et al*, 2007), these observations suggest that early embryonic stem cells may have alternative mechanisms to activate Cdk1. Trophoblasts also developed in the absence of Cdk7 but the small size of their nuclei suggests that they have reduced endoreplication cycles, a phenomenon also observed in *Mat1* knockout embryos (Rossi *et al*, 2001).

Selective inactivation of *Cdk7*^{lox} alleles in skin during embryonic development resulted in defective Cdk phosphorylation, hypophosphorylation of the pocket proteins and proliferative arrest. However, phosphorylation of the Ser5 residue of RNA pol II was unaffected, thus extending the results obtained with cultured MEFs. Skin areas lacking Cdk7 displayed an altered differentiation pattern and a severe reduction in the number of hair follicles. Interestingly, adjacent regions in which the *Cdk7*^{lox} alleles had not undergone genetic recombination exhibited a hyperplastic phenotype, most likely a compensatory response to the defects present in the neighbouring hypoplastic areas.

Widespread loss of Cdk7 expression in young adult mice did not lead to an obvious phenotype. Interestingly, low proliferative organs such as liver, kidney or brain displayed normal histology and the animals maintained standard levels of physiological parameters in spite of extensive loss of Cdk7 expression in these tissues thus, suggesting that Cdk7 is not essential to maintain cellular homeostasis in low proliferating organs. In contrast, highly proliferative tissues such as intestine or skin retained Cdk7 expression in most of their cells. These observations were not due to inefficient recombination of the *Cdk7*^{lox} alleles as the heterozygous *Cdk7*$^{+/lox}$; Ub-CreERT2$^{+/T}$ mice displayed a widespread occurrence of recombined *Cdk7*^{mut} alleles. Instead, these findings must be a consequence of the efficient replacement of cells lacking Cdk7 by cells derived from a pool of stem cells that had retained expression of this kinase, thereby maintaining normal organ function. This hypothesis would predict that as mice age, these pools of Cdk7-expressing stem cells should become exhausted. Indeed, *Cdk7*$^{lox/lox}$;Ub-CreERT2$^{+/T}$ mice exposed to a continuous tamoxifen diet developed a variety of age-related phenotypes including diffuse alopecia, pervasive hair-greying and kyphosis. Moreover, these mice underwent premature death with $<20\%$ of the animals surviving more than a year.

Detailed examination of their tissues revealed defects characteristic of premature aging such as decreased bone mineral content, accumulation of fat cells in the bone marrow and presence of hepatocytes positive for phosphorylated histone γ-H2AX. In addition, *Cdk7*$^{lox/lox}$;Ub-CreERT2$^{+/T}$ mice presented hypoplastic crypts and villi in the small intestine, as well as progressive nephropathy and severe medullary calcification in their kidneys. Their skin also presented phenotypic marks associated with premature aging including reduced dermal thickness, loss of subcutaneous adipose layer and transformation of follicular epithelium into sebaceous glands. Moreover, the bulge region of the hair follicles had limited numbers of progenitor cells. Finally, the substantial increase in the percentage of short telomeres in the epidermis (Figure 7) reinforces the hypothesis that the stem cell pool in adult *Cdk7*$^{lox/lox}$;Ub-Cre$^{+/T}$ animals has endured an extended proliferative period.

Activation of tissue renewal in adult mice devoid of Cdk7 relies entirely on physiological signals. Therefore, the mobilization of progenitor pools required to maintain homeostasis in highly proliferative tissues upon Cdk7 elimination may provide a useful tool for the identification of adult stem cell niches by lineage tracing experiments. Finally, Cdk7 has been considered a putative therapeutic target to inhibit tumour development (Fisher, 2005). The maintenance of normal physiological parameters by critical tissues such as liver, kidney or the endocrine pancreas in the absence of Cdk7 suggests that Cdk7 inhibitors may not cause a significant toxicity, providing that they are not administered for long periods of time. Yet, the potential use of such inhibitors may depend on the relative ability of adult stem cells to replenish highly proliferating tissues versus cancer stem cells to replace Cdk7-deficient tumour cells. Conditional ablation of the *Cdk7*^{lox} alleles described here in well-defined mouse tumour models should help to evaluate the therapeutic potential of Cdk7 as a cancer target.

Materials and methods

Mouse strains

All animal experiments were approved by the CNIO Ethical Committee and performed in accordance with the guidelines stated in the International Guiding Principles for Biomedical Research Involving Animals, developed by the Council for International Organizations of Medical Sciences (CIOMS). *Cdk7*$^{+/loxfrt}$ mice were generated from an ES cell clone (Ref D032B11) purchased from the German Gene Trap Consortium (Schnütgen *et al*, 2005). The *Cdk7*^{loxfrt} allele carries the genetrap vector in the active orientation and prevents *Cdk7* gene expression (Supplementary Figure 1). To generate the *Cdk7*$^{+/lox}$ strain, *Cdk7*$^{+/loxfrt}$ mice were crossed to the ACTB-FLPe tool strain that expresses the FLPe recombinase in the germ line to invert the genetrap to allow reexpression of the targeted allele (Supplementary Figure 1; Rodríguez *et al*, 2000). *Cdk7*$^{+/lox}$ and *Cdk7*$^{lox/lox}$ mice were crossed to the K5-Cre and Ub-CreERT2 transgenic strains to eliminate the expression of *Cdk7* alleles via Cre-mediated recombination. This allele has been designated as *Cdk7*^{mut} to indicate that it retains all the *Cdk7* genomic sequences, yet it does not produce detectable *Cdk7* transcripts or Cdk7 protein

(Supplementary Figure 1C and Figure 1, respectively). To induce CreERT2-mediated recombination in *Cdk7*$^{lox/lox}$;Ub-CreERT2$^{+/T}$ mice, animals were fed *ad libitum* with tamoxifen-containing diet (Harland-Tekald CRD TAM^{400}) starting after weaning (P21-P30). The K5-Cre and Ub-CreERT2 strains have been described elsewhere (Tarutani *et al*, 1997; Ruzankina *et al*, 2007).

Genotyping

Primers used for genotyping these *Cdk7* alleles included primers ExN (5′-GTTCCTTACCCCATCATCTGTCAC-3′) and Ex12RC (5′-GTTG CCCAGGGGGAATAAAGG-3′) for amplification of the wild-type *Cdk7* allele (310 bp); primers IntL (5′-GGAGACTCTTGCAAAAA CTAACCCCACCTC-3′) and B40 (5′-GGGTCGATGGTGATGCTTGGCA ATTC-3′) for amplification of the *Cdk7*^{loxfrt} allele (650 bp); and primers ExN and B48 (5′-TCCCACTGTCCTTTCCTAATAA-3′) for amplification of the *Cdk7*^{lox} allele (852 bp). Primers CreF (5′-CCC GCAGAACCTGAAGATGT-3′) and CreR (5′-GTTCGAACGCTAGAGCC TGTTT-3′) were used to genotype the K5-Cre and Ub-CreERT2 transgenes (220 bp). All alleles were amplified as follows: 94°C for 2 min; 35 cycles at 94°C for 30 s; 60°C for 30 s; 72°C for 30 s and then followed by 72°C for 10 min.

Real-time PCR analysis

Cdk7 mRNA levels were assayed using Power SYBR® Green PCR Master Mix (Applied Biosystems). Primers detecting Cdk7 wild-type mRNA: Cdk7-FW1 (located in exon 2, 5′-CAGTTTGCGACGGTCTA-TAAGG-3′), Cdk7-RV4 (located in exon 3, 5′-GCTTTATCTCCCTT-AAGGCTGTTC-3′). β-Actin mRNA levels were used as internal controls. The following β-Actin mRNA primers were used: β-Actin-QRT5 (5′-GACGGCCAGGTCATCACTATTG-3′) and β-Actin-QRT3 (5′-AGGAAGGCTGGAAAAGAGCC-3′).

In vivo imaging

Bone mineral analysis from total body imaging was carried out with the help of dual-energy X-ray absorptiometry (DEXA) using a Lunar PIXImus Densitometer (GE Medical Systems). Acquisition time was 5 min with 2% isofluorane as inhalatory anaesthesia. The analysis of bone mineral density was performed using a manual region of interest (ROI) in the femur. For the analysis of the trabecular area, the femur was imaged using the eXplore Locus micro-CT scanner (GE Healthcare). The reconstructed images were viewed and analysed using MicroView 2.2 Advanced Bone Analysis software (ABA, GE Healthcare). The isotropic resolution was set to 45 μm. The micro-CT image acquisition consisted of 400 projections collected in one full rotation of the gantry in ∼10 min. The X-ray tube settings were 80 kV and 450 μA. The resulting raw data were reconstructed to a final image volume of $875 \times 875 \times 465$ slices at (93 μm^3) voxel dimensions. The reconstructed slices were output in the CT manufacturer's raw format and were corrected to Hounsfield units.

Immunofluorescence

Embryos were fixed with cold methanol during 15 min at −20°C, washed in PBS containing 4% BSA, blocked with PBS containing 4% BSA for 1 h and incubated with primary antibodies for 90 min at 37°C. Secondary antibodies carrying Alexa 488, 594 or 647 fluorochromes were obtained from Molecular Probes (Invitrogen). Embryos were transferred to Vectashield mounting medium (Vector) on μClear plates (Greiner) for image acquisition. Images were obtained using a confocal ultra-spectral microscope (Leica TCS-SP5-AOBS-UV). For trophoblast analysis, embryos were grown on μClear plates and were allowed to hatch. Nuclear volumes were calculated on confocal images using ImageJ software. Antibodies used included anti Cdk7 (sc-7344, Santa Cruz), Nanog (NB100-588, Novus) and BrdU (RPN202, GE Healthcare). Nuclei were stained with Hoechst 33342 (Invitrogen). Embryos were genotyped by nested PCR, following immunofluorescence staining and confocal analysis.

Cell culture assays

MEFs were isolated from E13.5 embryos of the corresponding genotype and propagated according to standard 3T3 protocols. For proliferation assays, 500 cells were plated in 96-well plates in DMEM supplemented with 10% fetal bovine serum and their growth rate determined by the MTT 'Cell proliferation kit' (Roche). To obtain *Cdk7*$^{mut/mut}$ MEFs, *Cdk7*$^{lox/lox}$ MEFs were infected with Ad-Cre (Supplementary Figure 1). All *Cdk7*$^{mut/mut}$ MEFs were positive upon X-Gal staining demonstrating that the genetrap is integrated in the active orientation. These MEFs failed to express detectable levels of Cdk7 protein. (Figure 1A and Supplementary Figure 2C). Adenoviral infections were performed using a MOI of 150. The Cdk7^{T170A}, Cdk7^{K41A}, Cdk4^{T174E}, Cdk6^{T177E}, Cdk2^{T160E} and Cdk1^{T161E} mutants were generated using the QuickChange site directed mutagenesis kit (Stratagene) and delivered by retroviral infection. For labelling of cellular proteins, 5×10^5 MEFs were seeded in triplicate in six-well plates 1 week after infection with Ad-GFP or Ad-Cre particles and serum starved for 72 h. MEFs were then incubated in the presence of 100 μ Ci ^{35}S-protein labelling mix (Amersham) for 2 and 4 h. Cells were washed twice with PBS and lysed with 1% Triton X-100 PBS buffer. Total protein was precipitated from lysates with 10% TCA. Pellets were subjected to liquid scintillation counting to measure incorporated radioactivity.

Gene expression analysis

MEFs were infected with Ad-Cre or Ad-GFP particles and harvested after 1 week in culture. Cells were tripsinized and re-plated as necessary to maintain sub-confluent cultures. RNA was extracted using RNeasy kit (Quiagen). RNA integrity was assayed by Lab-chip technology on an Agilent 2100 Bioanalyzer. One microgram per sample was labelled with 'Two-Color Microarray-Based Gene Expression Analysis (Agilent)' and purified with silica-based RNeasy spin columns (Qiagen). Samples were hybridized to Mouse WMG 4×44K (Agilent). Microarrays were scanned on a G2565C DNA microarray scanner (Agilent). Images were quantified using Agilent Feature Extraction Software (version 10.1.1). Microarray background subtraction was carried out using normexp method. To normalize the data set, we performed loess within arrays normalization and quantiles between arrays normalization. Differentially expressed genes were obtained by applying linear models with R limma package (Smyth *et al*, 2005) available at the Bioconductor Project (http://www.bioconductor.org). To account for multiple hypotheses testing, the estimated significance level (*P* value) was adjusted using Benjamini & Hochberg false discovery rate (FDR) correction. Those genes with FDR <0.05 were selected as differentially expressed between Ad-Cre- and Ad-GFP-infected cultures. GSEA was applied using annotations from a curated version of Biocarta, KEGG (Reactome, GenMapp). Custom gene sets were built from literature (Bracken *et al*, 2004; Eisenberg and Levanon, 2003). Genes were ranked based on limma-moderated *t* statistic. After Kolmogorov–Smirnoff testing, those gene sets showing FDR <0.25, a well-established cut-off for the identification of biologically relevant gene sets (Subramanian *et al*, 2005), were considered enriched between classes under comparison. Microarray experiments data have been deposited at the NCBI Gene Expression Omnibus (GEO) database and are freely accessible: GSE36050.

Histopathology and immunostaining

For routine histological analysis, tissues were fixed in 10%-buffered formalin (Sigma) and embedded in paraffin. Immunohistochemical staining was performed on 3–4 μm paraffin sections. Antibodies used included those elicited against Cdk7 (sc-7344, Santa Cruz), P-Thr160-Cdk2 (2561, Cell Signalling), P-Ser5-RNA pol II (H14, Covance), P- Ser807/811-pRb (9308, Cell Signalling), Insulin (A0564, Dako), Glucagon (G2654, Sigma) and phosphorylated γ-H2AX (05-636, Millipore). Immunofluorescence staining of skin sections was performed with the following antibodies: Cdk7 (sc-7344, Santa Cruz), keratin K5 (PRB-160, Covance), keratin K6 (PRB-169, Covance), keratin K10 (M7002, Dako), loricrin (PRB-145, Covance) and PCNA (PC10, Thermo Scientific).

Protein analysis

Cell pellets were processed for western blotting and kinase assays, as previously described (Santamaría *et al*, 2007). Primary antibodies used included those elicited against Cdk7 (sc-7344, Santa Cruz), Cdk2, Cdk4 and Cdk6 (our own rabbit polyclonals), P-Thr160-Cdk2 (2561, Cell Signalling), Cdk1 (sc-54, Santa Cruz), P-Thr161-Cdk1 (9114, Cell Signalling), Mat1 (sc-13142, Santa Cruz), CycH (2927, Cell Signalling), pRb (554136, BD Pharmingen), P-Ser807/811-pRb (9308, Cell Signalling), RNA pol II (8WG16, Covance), p-Ser5-RNA pol II (H14, Covance) and GAPDH (Sigma).

Supplementary data
Supplementary data are available at *The EMBO Journal* Online (http://www.embojournal.org).

Acknowledgements

We thank C Timón, MC González, M San Román and R Villar for their excellent technical assistance. We thank EJ Brown (Abramson Family Cancer Research Institute, University of Pennsylvania School of Medicine, Philadelphia) and J Takeda (Osaka University) for kindly providing the Ub-CreERT2 and K5-Cre transgenic mice, respectively. Work in the laboratory of MB was supported by grants from the EU-Framework Programme (LSHG-CT-2007-037665), European Research Council (ERC-AG/250297-RAS AHEAD), Spanish Ministry of Science and Innovation (MICINN) (SAF2006-11773 and CSD2007-00017), Autonomous Community of Madrid (GR/SAL/0587/2004 and S2006/BIO-0232) and *Fundación de la Mutua Madrileña del Automóvil*. MG was supported by an FPU fellowship (MICINN). Work in the laboratory of JMP was supported by grants from the MICINN (SAF2006-00121 and SAF2011-26122-C02-01), Autonomous Community of Madrid (S2006/BIO-0232) and Spanish Ministry of Health (ISCIII-RETIC RD06/0020/0029). MB is an AXA-CNIO Professor of Molecular Oncology.

Author contributions: DS and MB supervised the entire project and designed the experiments together with MG and JMP. DS and MB wrote the manuscript with comments from co-authors. MG generated and characterized all mouse strains and carried out most of the experiments. CS performed skin immunofluorescence studies. MC was responsible for histopathological analysis. DP and GG analysed microarray data. MAB and RS performed telomeric length analysis.

Conflict of interest

The authors declare no conflict of interest.

References

Berthet C, Aleem E, Coppola V, Tessarollo L, Kaldis P (2003) Cdk2 knockout mice are viable. *Curr Biol* **13:** 1775–1785

Blanpain C, Lowry WE, Geoghegan A, Polak L, Fuchs E (2004) Self-renewal, multipotency, and the existence of two cell populations within an epithelial stem cell niche. *Cell* **118:** 635–648

Bracken AP, Ciro M, Cocito A, Helin K (2004) E2F target genes: unraveling the biology. *Trends Biochem Sci* **29:** 409–417

Canela A, Vera E, Klatt P, Blasco MA (2009) High-throughput telomere length quantification by FISH and its application to human population studies. *Proc Natl Acad Sci USA* **104:** 5300–5305

Chuttani A, Gilchrest BA (1995) Aging. In *Handbook of Physiology*, Masoro EJ (ed) pp 309–324. Oxford Univ. Press, New York

Eisenberg E, Levanon EY (2003) Human housekeeping genes are compact. *Trends Genet* **19:** 362–365

Fisher RP (2005) Secrets of a double agent: CDK7 in cell-cycle control and transcription. *J Cell Sci* **118:** 5171–5180

Flores I, Blasco MA (2010) The role of telomeres and telomerase in stem cell aging. *FEBS Lett* **584:** 3826–3830

Flores I, Canela A, Vera E, Tejera A, Cotsarelis G, Blasco MA (2008) The longest telomeres: a general signature of adult stem cell compartments. *Genes Dev* **22:** 654–667

Haines DC, Chattopadhyay S, Ward JM (2001) Pathology of aging B6;129 mice. *Toxicol Pathol* **29:** 653–661

Harper JW, Elledge SJ (1998) The role of Cdk7 in CAK function, a retro-retrospective. *Genes Dev* **12:** 285–289

Hemann MT, Strong MA, Hao LY, Greider CV (2001) The shortest telomere, not average telomere length, is critical for cell viability and chromosome instability. *Cell* **107:** 67–77

Kim JB, Sharp PA (2001) Positive transcription elongation factor B phosphorylates hSPT5 and RNA polymerase II carboxyl-terminal domain independently of cyclin-dependent kinase-activating kinase. *J Biol Chem* **276:** 12317–12323

Korsisaari N, Rossi DJ, Paetau A, Charnay P, Henkemeyer M, Mäkelä TP (2002) Conditional ablation of the Mat1 subunit of TFIIH in Schwann cells provides evidence that Mat1 is not required for general transcription. *J Cell Sci* **115:** 4275–4284

Krishnamurthy J, Sharpless NE (2007) Stem cells and the rate of living. *Cell Stem Cell* **1:** 9–11

Larochelle S, Chen J, Knights R, Pandur J, Morcillo P, Erdjument-Bromage H, Tempst P, Suter B, Fisher RP (2001) T-loop phosphorylation stabilizes the CDK7-cyclin H-MAT1 complex *in vivo* and regulates its CTD kinase activity. *EMBO J* **20:** 3749–3759

Larochelle S, Pandur J, Fisher RP, Salz HK, Suter B (1998) Cdk7 is essential for mitosis and for *in vivo* cdk-activating kinase activity. *Genes Dev* **12:** 370–381

Lee KM, Miklos I, Du H, Watt S, Szilagyi Z, Saiz JE, Madabhushi R, Penkett CJ, Sipiczki M, Bähler J *et al* (2005) Impairment of the TFIIH-associated CDK-activating kinase selectively affects cell cycle-regulated gene expression in fission yeast. *Mol Biol Cell* **16:** 2734–2745

Lolli G, Johnson LN (2005) CAK-Cyclin-dependent activating kinase: a key kinase in cell cycle control and a target for drugs? *Cell Cycle* **4:** 572–577

Lyle S, Christofidou-Solomidou M, Liu Y, Elder DE, Albelda S, Cotsarelis G (1998) The C8/144B monoclonal antibody recognizes cytokeratin 15 and defines the location of human hair follicle stem cells. *J Cell Sci* **111:** 3179–3188

Malumbres M, Barbacid M (2005) Mammalian Cyclin-dependent kinases. *Trends Biochem Sci* **30:** 630–641

Matheu A, Maraver A, Klatt P, Flores I, Garcia-Cao I, Borras C, Flores JM, Viña J, Blasco MA, Serrano M (2007) Delayed ageing through damage protection by the Arf/p53 pathway. *Nature* **448:** 375–379

Moerman EJ, Teng K, Lipschitz DA, Lecka-Czernik B (2004) Aging activates adipogenic and suppresses osteogenic programs in mesenchymal marrow stroma/stem cells: the role of PPAR-gamma2 transcription factor and TGF-beta/BMP signaling pathways. *Aging Cell* **3:** 379–389

Ni Z, Schwartz BE, Werner J, Suarez JR, Lis JT (2004) Coordination of transcription, RNA processing, and surveillance by P-TEFb kinase on heat shock genes. *Mol Cell* **16:** 55–65

Ortega S, Prieto I, Odajima J, Martín A, Dubus P, Sotillo R, Barbero JL, Malumbres M, Barbacid M (2003) Cyclin-dependent kinase 2 is essential for meiosis but not for mitotic cell division in mice. *Nat Genet* **35:** 25–31

Palancade B, Bensaude O (2003) Investigating RNA polymerase II carboxyl-terminal domain (CTD) phosphorylation. *Eur J Biochem* **270:** 3859–3870

Patel SA, Simon MC (2010) Functional analysis of the Cdk7.cyclin H.Mat1 complex in mouse embryonic stem cells and embryos. *J Biol Chem* **285:** 15587–15598

Rodríguez CI, Buchholz F, Galloway J, Sequerra R, Kasper J, Ayala R, Stewart AF, Dymecki SM (2000) High-efficiency deleter mice show that FLPe is an alternative to Cre-loxP. *Nat Genet* **25:** 139–140

Rossi DJ, Londesborough A, Korsisaari N, Pihlak A, Lehtonen E, Henkemeyer M, Mäkelä TP (2001) Inability to enter S phase and defective RNA polymerase II CTD phosphorylation in mice lacking Mat1. *EMBO J* **20:** 2844–2856

Ruzankina Y, Pinzon-Guzman C, Asare A, Ong T, Pontano L, Cotsarelis G, Zediak VP, Velez M, Bhandoola A, Brown EJ (2007) Deletion of the developmentally essential gene ATR in adult mice leads to age-related phenotypes and stem cell loss. *Cell Stem Cell* **7:** 113–126

Santamaría D, Barrière C, Cerqueira A, Hunt S, Tardy C, Newton K, Cáceres JF, Dubus P, Malumbres M, Barbacid M (2007) Cdk1 is sufficient to drive the mammalian cell cycle. *Nature* **448:** 811–815

Satyanarayana A, Berthet C, Lopez-Molina J, Coppola V, Tessarollo L, Kaldis P (2008) Genetic substitution of Cdk1 by Cdk2 leads to embryonic lethality and loss of meiotic function of Cdk2. *Development* **135:** 3389–3400

Schnütgen F, De-Zolt S, Van Sloun P, Hollatz M, Floss T, Hansen J, Altschmied J, Seisenberger C, Ghyselinck NB, Ruiz P, Chambon P, Wurst W, von Melchner H (2005) Genomewide production of multipurpose alleles for the functional analysis of the mouse genome. *Proc Natl Acad Sci USA* **102:** 7221–7226

Smyth GK, Michaud J, Scott HS (2005) Use of within-array replicate spots for assessing differential expression in microarray experiments. *Bioinformatics* **21:** 2067–2075

Subramanian A, Tamayo P, Mootha VK, Mukherjee S, Ebert BL, Gillette MA, Paulovich A, Pomeroy SL, Golub TR, Lander ES, Mesirov JP (2005) Gene set enrichment analysis: a knowledge-based approach for interpreting genome-wide expression profiles. *Proc Natl Acad Sci USA* **102:** 15545–15550

Tarutani M, Itami S, Okabe M, Ikawa M, Tezuka T, Yoshikawa K, Kinoshita T, Takeda J (1997) Tissue-specific knockout of the mouse Pig-a gene reveals important roles for GPI-anchored proteins in skin development. *Proc Natl Acad Sci USA* **94:** 7400–7405

Wallenfang MR, Seydoux G (2002) cdk-7 is required for mRNA transcription and cell cycle progression in Caenorhabditis elegans embryos. *Proc Natl Acad Sci USA* **99:** 5527–5532

